

Holographic Entanglement Entropy and Complexity for D-Wave Superconductors

Yuanceng Xu,^{1,*} Yu Shi,² Dong Wang,³ and Qiyuan Pan^{3,†}

¹*Institute of Astrophysics, Central China Normal University, Wuhan, Hubei 430079, China*

²*School of Physics, Electronics and Intelligent Manufacturing,
Huaihua University, Huaihua, Hunan 418000, China*

³*Key Laboratory of Low Dimensional Quantum Structures
and Quantum Control of Ministry of Education,
Synergetic Innovation Center for Quantum Effects and Applications,
and Department of Physics, Hunan Normal University, Changsha, Hunan 410081, China*

(Dated: September 27, 2022)

Abstract

By using the RT formula and the subregion CV conjecture respectively, we numerically investigate the holographic entanglement entropy (HEE) and holographic subregion complexity (HSC) for two holographic d-wave superconducting models with backreactions. We find that both the HEE and HSC can be used as good probes to these two d-wave superconducting phase transitions. The HEE of superconducting phase is always lower than that of the normal phase due to the condensation of degrees of freedom below the critical temperature T_c . However, for the HSC, it behaves differently and interestingly, which depends on both the strip-width L_x and backreaction κ .

* xyc@mails.ccmu.edu.cn

† panqiyuan@hunnu.edu.cn

I. INTRODUCTION

The anti-de Sitter/conformal field theories (AdS/CFT) duality (or gauge/gravity duality) provides us with a powerful tool for studying strongly coupled quantum systems. The gauge/gravity duality is originated from the study of superstring theory. More specifically, Maldacena proposed that the Type *IIB* string theory (*D3* branes) on $(AdS_5 \times S^5)_N$ with some appropriate boundary conditions (and possibly also some boundary degrees of freedom) is dual to $4d \mathcal{N} = 4 U(N)$ Super-Yang-Mills theory in the large N limit [1–3]. In the past two decades, the gauge/gravity duality has been widely applied to various fields of physics. Two of the more well-known and successful areas are quantum chromodynamics (QCD) [4–6] and condensed matter physics (CMP) [7–9]. This paper mainly introduces the holographic duality of superconductivity in condensed matter physics. Since the first discovery of the high temperature superconductors (HTS) [10] in 1986, people have tried to propose various theories for their electron pairing mechanism. Even the famous BCS theory has failed to provide a reasonable explanation for the HTS systems with strong coupling. As a new powerful tool, the gauge/gravity duality [1–3] can be used to study strong coupled systems. In 2008, Gubser pointed out that the spontaneous $U(1)$ symmetry breaking by bulk black holes which can be used to investigate the superconductor/conductor phase transitions in the dual CFTs [11]. Then Hartnoll et al. built the first holographic superconducting model [12]. Indeed, using the gauge/gravity duality, such a simple model can yield condensed curves, which is similar to results of BCS theory. In addition to the holographic duality of s-wave superconductor mentioned above, the authors [13, 14] established a holographic duality of p-wave superconductor by putting a $SU(2)$ Yang-Mills field around the AdS black hole. However, most of the previous studies focused on the s-wave and p-wave order parameters. In fact, many experiments [15–18] have found that most HTS materials are d-wave superconductors, which means that the orbital angular momentum of electron pair (Cooper pair) equal to two. Because of a possible relationship with cuprates, it would be an important but challenging task to construct a complete and self-consistent (no other unphysical degrees of freedom) holographic dual theory of d-wave superconductivity. A truncated model which has sufficient ingredients to catch main features of d-wave superconductors was proposed by the authors (CKMWY) in the paper [19]. They replaced the scalar field in holographic s-wave superconductors with a tensor field. A d-wave state could be

described by a 3×3 symmetric traceless tensor which has 5 components naturally. When the time component was considered, this symmetric traceless tensor could be expressed as $B_{\mu\nu}(\mu, \nu = 0, 1, 2, 3)$ with $B_{\mu\nu} = B_{\nu\mu}$ and $B_{\mu}^{\mu} = 0$. Although this toy model has some features of d-wave superconductor, it's still an incomplete theory and contains the spurious degrees of freedom that may cause the instability. Inspired by the early studies of a neutral, massive spin-two field in a flat background, the authors (BHRY) [20] found another toy model for a charged spin-two field in an asymptotical AdS geometry which could be used to describe the d-wave order parameter. Fortunately, the action they wrote down has the correct number of propagating degrees of freedom, and it is ghost-free and stable. In the context of holographic superconductors, it was often work in the probe limit [12] to simplify the calculations and catch the typical properties of condensation. However, sometimes we have to consider the effect of a full backreaction on the metric when calculating some particular quantities like the HEE and the HSC in holographic superconductors. In this case, the constraint equations are derived from the general form of the Einstein field equation $R_{\mu\nu} - \frac{1}{2}g_{\mu\nu}R + \Lambda g_{\mu\nu} = \kappa^2 T_{\mu\nu}$. For generic values of $F_{\mu\nu}$, this model also has the unwanted feature of non-hyperbolic or non-causal propagation [21]. Fortunately, these problems can be corrected by adding higher order of $F_{\mu\nu}$ to the lagrangian terms. One motivation for this paper is, when keeping both the conformal dimension Δ_+ and backreaction κ corresponding to two d-wave superconducting models the same respectively, to compare the critical temperature of the phase transition between these models.

In addition to its wide application in CMP and QCD, the gauge/gravity duality has been recently extended in quantum information physics (QIP), such as the entanglement entropy and the computational complexity. Considering a quantum system divided into two subsystems A and B, the total hilbert space can be written as the direct product of two subspaces $\mathcal{H}_{tot} = \mathcal{H}_A \otimes \mathcal{H}_B$. Then the entanglement entropy of subsystem A can be defined by von Neumann entropy, $S_A = -tr_A(\rho_A \log \rho_A)$ with the reduced density matrix $\rho_A = tr_B(\rho_{tot})$. The entanglement entropy can be used to measure how closely entangled (or how “quantum”) a given wave function is. It's very difficult to calculate the entanglement entropy of arbitrary submanifolds A directly in higher dimensional QFT. Fortunately, a holographic interpretation of entanglement entropy in CFT was proposed by S. Ryu and T.

Takayanagi [22, 23]

$$S_A = \frac{Area(\gamma_A)}{4G_N}, \quad (1)$$

where $Area(\gamma_A)$ is the area of the static minimal surface in AdS spacetime whose boundary is given by ∂A . G_N is the Newton constant. Indeed, the authors [22, 23] investigated the area of a one-dimensional minimal surface (i.e, the length of a geodesic) on the AdS_3 boundary, and the entropy obtained by the holographic interpretation is exactly consistent with the result of CFT_2 , i.e, $S_A = \frac{c}{3} \cdot \log \left[\frac{L}{\pi a} \sin \left(\frac{\pi l}{L} \right) \right]$, even including the (universal) coefficients. Inspired by these two papers [24, 25], where the HEE in s-wave and p-wave superconductors was studied by Albash and Cai et. al. respectively, in this paper, we would like to investigate the HEE in holographic d-wave superconducting models. As mentioned above, most high temperature superconducting materials are d-wave superconductors. Therefore, it is necessary to investigate whether the entanglement entropy can be used to probe d-wave superconducting phase transitions. If so, then we can say that the HEE can be used to detect *all* superconducting phase transitions.

Another information-theoretic quantity, the computational complexity [26] was related to a gravitational concept within the context of AdS/CFT correspondence. Computational complexity is a measure of how difficulty it is to carry out an unitary operation U . More specifically, it's defined by the minimum number of "basic" unitary operations ("gates") required to implement the operation U . For example, according to the AdS/CFT duality, the state $|\psi(t_L, t_R)\rangle$ on the boundary of the analytic eternal two-sided AdS-Schwarzschild black hole is determined by what we called the thermofield double $|TFD\rangle$ state. The CV-conjecture (Complexity/Volume conjecture) [26, 27] proposes that the complexity of the state $|\psi(t_L, t_R)\rangle$ can be obtained by the maximum spatial volume V of ERBs (Einstein-Rosen bridges) which connect the boundary of the left and right black hole. Another improved conjecture, the CA-conjecture (Complexity/Action conjecture) [28, 29] proposes that the complexity of a state is given by the classical action \mathcal{A} of a region which is called the Wheeler-DeWitt(WDW) patch in the Penrose diagram. Unlike the HEE, which exists only in the bulk geometry outside of the black hole, the holographic complexity (HC) allows us to delve into the inside of the black hole and reveal the physics behind the event horizon. However, motivated by the HEE and the HC, the volume enclosed by the minimal hypersurface and infinite boundary in the bulk may also define a complexity which is called

holographic subregion complexity (HSC) [30]

$$\mathcal{C}_A = \frac{V(\gamma_A)}{8\pi L G_N}, \quad (2)$$

where L is the AdS radius and G_N is Newton's constant. It's worth noting that, due to the metric is divergent on the infinite boundary of an asymptotic AdS geometry, to regulate this quantity, we need to put a UV cutoff $\epsilon = \frac{1}{r}$ near the boundary $r = \infty$ just like we did in the HEE. One can find the universal term of the HSC C_u by subtracting the diverging term from the total complexity. The HSC in s-wave and p-wave superconducting models has been studied [31–33]. In this paper, we would like to investigate the HSC as defined in Eq. 2 above in d-wave superconductors.

Another research motivation of this paper comes from the analysis of some existing results in the literature [31, 32, 34]. In Ref. [31], the authors claimed that the difference between the HEE (or the HSC) of superconducting phase and that of normal phase becomes larger as the value of backreaction κ becomes larger. Their investigation clarifies the conflicting and shows that the HSC does not behave in the same way as the HEE. More specifically, they found that the HEE S_u increases with the increase of T/μ , while the HSC C_u decreases with the increase of T/μ . Indeed, our results also show that the HEE does have such a similar property, but the behavior of HSC is more complicated and determined by the strip-width L_x of subregion and the value of backreaction κ . Although the authors there studied one-dimensional holographic s-wave superconductors, we believe that these two models are still comparable because the equations of motion of the d-wave superconductors are similar to those of the s-wave superconductors. Another thing that's worth noting is that in Ref. [31], the HSC of superconducting phase is larger than that of normal phase and decreases with the increase of the temperature T . While the authors of Ref. [34] claimed that the superconducting phase always has a smaller complexity than the normal phase below the critical temperature. Although the latter considers the general CV-conjecture (Complexity/Volume conjecture) [26, 27], it seems that there are something ambiguous about the behavior of complexity that needs further investigation. Our results show that when the backreaction κ^2 is larger than a certain critical value, or the strip-width $L_x\sqrt{\rho}$ of the boundary subsystem is smaller than a certain critical value, the HSC in the superconducting phase is larger than that in the normal phase, and vice versa, although the physical mechanisms involved are not well understood.

This paper is organized as follows: In Sec. II, we briefly review the two holographic d-wave superconducting models respectively and obtain the critical temperatures of phase transition under three different values of the backreaction. In Sec. III, we study the HEE and HSC of two holographic d-wave superconducting models respectively. In Sec. IV, we summarize and discuss our results.

II. D-WAVE SUPERCONDUCTORS

A. CKMWY D-Wave Superconductor

In this section, we will briefly introduce the d-wave superconductor which is described by the background geometry of a black hole coupled with a symmetric, traceless second-rank tensor field $B_{\mu\nu}$ and a U(1) gauge field. The total action takes the following form ¹ [19]

$$S = \int d^4x \sqrt{-g} \left[\frac{1}{2\kappa^2} (R - 2\Lambda) - \frac{1}{4} F_{\mu\nu} F^{\mu\nu} - (D_\mu B_{\nu\gamma})^* D^\mu B^{\nu\gamma} - m^2 B_{\mu\nu}^* B^{\mu\nu} \right], \quad (3)$$

where $\kappa^2 = 8\pi G_N$ is the gravitational coupling. R is the Ricci scalar and Λ is a negative cosmological constant ($\Lambda = -3/L^2$) with the AdS radius L . $F_{\mu\nu} = \nabla_\mu A_\nu - \nabla_\nu A_\mu$ is the Maxwell field strength. $B_{\mu\nu}$ is a symmetric traceless tensor with the charge q and mass m respectively. $D_\mu = \nabla_\mu - iqA_\mu$ is the covariant derivative in curved spacetime. In order to study the fully backreacted holographic superconductor, we consider a planar Schwarzschild-AdS ansatz

$$ds^2 = -f(r)e^{-\chi(r)} dt^2 + \frac{dr^2}{f(r)} + \frac{r^2}{L^2} (dx^2 + dy^2). \quad (4)$$

The Hawking temperature of this black hole (4), which will be interpreted as the temperature of the dual CFT, is given by

$$T = \left. \frac{e^{-\chi/2} f'}{4\pi} \right|_{r=r_+}. \quad (5)$$

For the convenience of calculation, we change the above metric into the following form after the coordinate transformation $r = r_+/z$. In the rest of the calculation, we're going to set

¹ It's worth noting that we've already used the familiar form for the material fields \mathcal{L}_m by the rescaling $B_{\mu\nu} \rightarrow \frac{qB_{\mu\nu}}{L}$ and $A_\mu \rightarrow \frac{qA_\mu}{L}$.

$r_+ = 1$ ². At this time, $z = 0$ is the boundary where the dual d-wave superconductor lives on,

$$ds^2 = -f(z)e^{-\chi(z)}dt^2 + \frac{dz^2}{z^4 f(z)} + \frac{1}{z^2 L^2} (dx^2 + dy^2). \quad (6)$$

The d-wave superconductor condensate on the $x - y$ plane of the boundary with translational invariance. The condensate change its sign under every $\pi/2$ rotation on the $x - y$ plane and the rotational symmetry is broken down to $Z(2)$. Considering these characteristics and in order to simplify the equations of motion as much as possible, we consider two ansatzes that the spatial components of symmetric traceless tensor field are given by $B_{\mu\nu}$: $B_{xx} = -B_{yy} = \psi(z)/(\sqrt{2}z^2)$ or $B_{xy} = B_{yx} = \psi(z)/(\sqrt{2}z^2)$. If either of the two ansatzes is chosen, the other must be vanished. Two ansatzes are equivalent under a $\theta = \pi/4$ rotation on the $x - y$ plane and the equations of motion for both ansatzes are the same

$$\begin{pmatrix} B_{xx} \\ B_{xy} \end{pmatrix} \rightarrow \begin{pmatrix} \cos 2\theta & -\sin 2\theta \\ \sin 2\theta & \cos 2\theta \end{pmatrix} \begin{pmatrix} B_{xx} \\ B_{xy} \end{pmatrix}. \quad (7)$$

We just select one of them for the tensor field $B_{\mu\nu}$ and gauge field A_μ , i.e,

$$B_{xx} = -B_{yy} = \frac{\psi(z)}{\sqrt{2}z^2}, \quad A_\mu dx^\mu = \phi(z)dt. \quad (8)$$

After the variation of the action (3), the equations of motion can be easily obtained³

$$\psi''(z) + \psi'(z) \left[\frac{f'(z)}{f(z)} - \frac{\chi'(z)}{2} \right] + \psi(z) \left[\frac{q^2 e^{\chi(z)} \phi(z)^2}{z^4 f(z)^2} - \frac{m^2}{z^4 f(z)} - \frac{2}{z^2} \right] = 0, \quad (9)$$

$$\phi''(z) + \frac{\chi'(z)\phi'(z)}{2} - \frac{2q^2\phi(z)\psi(z)^2}{z^4 f(z)} = 0, \quad (10)$$

$$\chi'(z) - 2\kappa^2 z \left\{ \psi'(z)^2 + \psi(z)^2 \left[\frac{2}{z^2} + \frac{q^2 e^{\chi(z)} \phi(z)^2}{z^4 f(z)^2} \right] \right\} = 0, \quad (11)$$

$$f'(z) - \frac{f(z)}{z} + \frac{3}{z^3} - \kappa^2 z \left\{ \frac{e^{\chi(z)} \phi'(z)^2}{2} + f(z) \psi'(z)^2 + \psi(z)^2 \left[\frac{m^2}{z^4} + \frac{q^2 e^{\chi(z)} \phi(z)^2}{z^4 f(z)} + \frac{2f(z)}{z^2} \right] \right\} = 0. \quad (12)$$

Without loss of generality, we will set $q = 1$ and keep κ^2 finite when we take the backreactions into account⁴. Notice that these equations of motion are very similar to those for s-wave

² This is allowed because we have the scaling symmetry $r \rightarrow br$, $(t, x, y) \rightarrow b^{-1}(t, x, y)$, $f \rightarrow b^2 f$, $\phi \rightarrow b\phi$.

³ Notice that we've hidden the AdS radial L in the above equations of motion, since we've taken $L = 1$.

This is allowed because we have the scaling symmetries $L \rightarrow aL$, $z \rightarrow a^{-1}z$, $t \rightarrow at$, $q \rightarrow a^{-1}q$.

⁴ If one re-scales the tensor field $B_{\mu\nu}$ and the gauge potential A_μ to $B_{\mu\nu} \rightarrow \frac{B_{\mu\nu}}{q}$ and $A_\mu \rightarrow \frac{A_\mu}{q}$ in the action, the tensor field and Maxwell field equations (9)–(10) will remain invariant, but the gravitational coupling coefficient κ^2 of the Einstein field equations (11)–(12) is re-scaled by $\kappa^2 \rightarrow \frac{\kappa^2}{q^2}$. One can fix the charge density $q = 1$ and vary κ which used to reflect the strength of the backreaction.

superconductors. We will numerically solve the above equations by using the shooting method. Firstly, we need to know not only the behavior of the equations of motion at the horizon, but also the behavior of those equations toward the asymptotical AdS boundary. Because of $f(z_h) = 0$ and $\phi(z_h) = 0$ ⁵ those fields equations can be expanded at the horizon ($z_h = 1$),

$$\begin{aligned}\psi(z) &= \psi_0 + \psi_1(1 - z) + \dots, \\ \phi(z) &= \phi_1(1 - z) + \dots, \\ f(z) &= f_1(1 - z) + \dots, \\ \chi(z) &= \chi_0 + \chi_1(1 - z) + \dots,\end{aligned}\tag{13}$$

where the coefficients ψ_0 , ϕ_1 and χ_0 are some constants. In order to obtain $\psi(z)$, $\phi(z)$, $\chi(z)$ and $f(z)$ that satisfy the asymptotic boundary conditions of the equations, we can solve the equations of motion (9)–(12) by performing the shooting method. Before that, we need to know the asymptotic behavior of the equations of motion near the AdS boundary ($z \rightarrow 0$),

$$\chi(z) \approx \chi_c, \quad f(z) \approx \frac{1}{z^2}, \quad \phi \approx \mu - \rho z, \quad \psi \approx z^{\Delta_-} \psi_- + z^{\Delta_+} \psi_+, \tag{14}$$

where $\Delta_{\pm} = \frac{3 \pm \sqrt{17 + 4m^2}}{2}$ with the BF bound $m^2 \geq -17/4$. If $\Delta_- \leq 0$ ($m^2 \geq -2$), the normalizability requires that ψ_- must vanish. According to the gauge/gravity dictionary, the coefficient ψ_+ corresponds to the vacuum expectation value of the operator dual to the components of the tensor field $B_{\mu\nu}$ and ψ_- is dual to a source for this operator. In this paper, we consider $m^2 = -1/4$ (i.e. $\Delta_- = -1/2$ and $\Delta_+ = 7/2$). In order to get the metric (6) back to the standard AdS metric at the boundary, let's take constant $\chi_c = 0$ ⁶. Here μ is interpreted as the chemical potential and ρ as the charge density in the boundary theory. The condensate of the tensor operator $\langle \mathcal{O}_{ij} \rangle$ in the boundary field theory dual to the field $B_{\mu\nu}$ is given by

$$\langle \mathcal{O}_{ij} \rangle = \begin{pmatrix} \psi_+ & 0 \\ 0 & -\psi_+ \end{pmatrix}. \tag{15}$$

In Fig. 1(a), we plotted the critical temperature of the superconducting phase transition as a function of the backreactions. It was easy to see that the critical temperature decreases

⁵ To keep the norm of the gauge potential $A_\mu A^\mu = g^{tt} \phi^2$ finite at the horizon, the gauge potential ϕ must vanish.

⁶ This is allowed by the rescaling symmetry $e^x \rightarrow a^2 e^x$, $\phi \rightarrow \phi/a$, $t \rightarrow at$ for a particular value a .

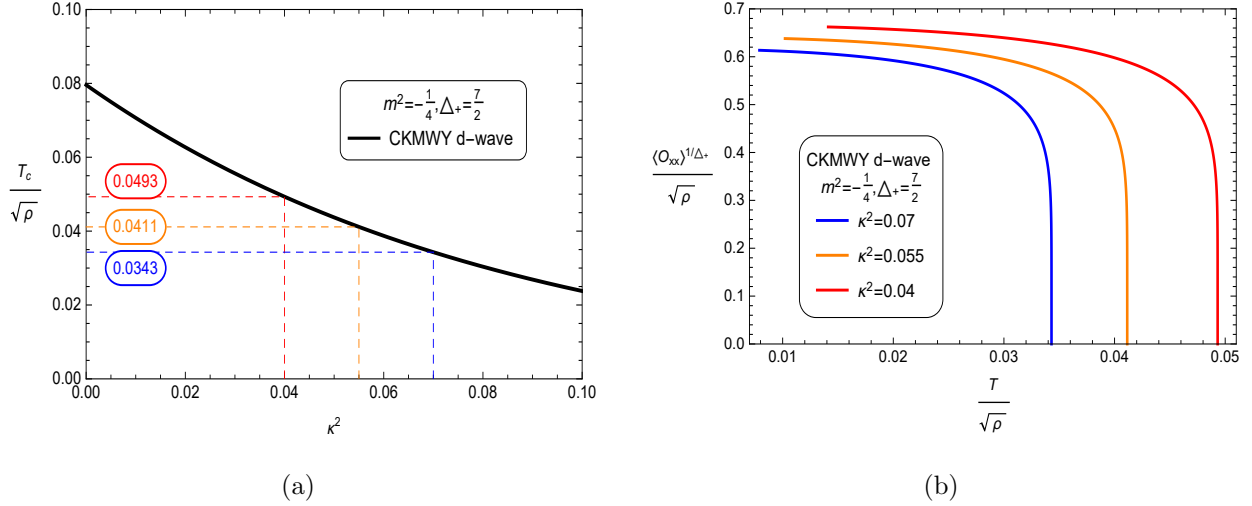


FIG. 1. The left figure depicts the change of critical temperature with backreaction κ^2 for $m^2 = -1/4$ in the CKMWY d-wave superconducting model. The right figure is the condensate as a function of temperature. Different color solid lines correspond to different backreaction values, the critical temperatures are $T_c/\sqrt{\rho} = 0.0343$ (blue: $\kappa^2 = 0.07$), $T_c/\sqrt{\rho} = 0.0411$ (orange: $\kappa^2 = 0.055$) and $T_c/\sqrt{\rho} = 0.0493$ (red: $\kappa^2 = 0.04$) respectively.

with the increase of the backreactions monotonically. Our results show that the stronger backreactions will make the operator to condense more difficult not only in s-wave superconductors [35, 36], but also in d-wave superconductors [37]. In Fig. 1(b), the condensations of the operator $\langle \mathcal{O}_{xx} \rangle$ for some backreactions were investigated. One can fit these curves near the critical point and observe that the expected value of the operator behaves like $\langle \mathcal{O}_{xx} \rangle \sim (T_c - T)^{1/2}$, which implies that the d-wave superconducting phase transition is a second order phase transition with the exponent $1/2$.

Finally, it is important to emphasize that the physical quantities that we want to obtain are independent of the scaling scale. Notice that, according to the scaling symmetry

$$(t, z, x, y) \rightarrow b^{-1}(t, z, x, y), \quad f \rightarrow b^2 f, \quad \phi \rightarrow b\phi, \quad (16)$$

the quantities T, μ, ρ and $\langle \mathcal{O}_{xx} \rangle$ scale as

$$T \rightarrow bT, \quad \mu \rightarrow b\mu, \quad \rho \rightarrow b^2\rho, \quad \langle \mathcal{O}_{xx} \rangle \equiv \psi_+ \rightarrow b^{\Delta_+}\psi_+. \quad (17)$$

Therefore, to study the physics, it is useful to make these quantities dimensionless, i.e., $T/\sqrt{\rho}, \langle \mathcal{O}_{xx} \rangle^{1/\Delta_+}/\sqrt{\rho}$.

B. BHRY D-Wave Superconductor

With the same strategy, in this section, we study the effect of backreactions on the d-wave model proposed by Benini et. al. (BHRY). This holographic model with a symmetric tensor field $\varphi_{\mu\nu}$ and a U(1) gauge field A_μ is described by the following action [20]

$$S = \int d^4x \sqrt{-g} \left\{ \frac{1}{2\kappa^2} \left(R + \frac{6}{L^2} \right) + \mathcal{L}_m \right\}, \quad (18)$$

with

$$\begin{aligned} \mathcal{L}_m = & -\frac{1}{4} F_{\mu\nu} F^{\mu\nu} - |D_\rho \varphi_{\mu\nu}|^2 + 2|D_\mu \varphi^{\mu\nu}|^2 + |D_\mu \varphi|^2 - (D_\mu \varphi^{\mu\nu} D_\nu \varphi + c.c.) - m^2(|\varphi_{\mu\nu}|^2 - |\varphi|^2) \\ & + 2R_{\mu\nu\rho\lambda} \varphi^{\mu\rho} \varphi^{\nu\lambda} - \frac{1}{4} R |\varphi|^2 - iq F_{\mu\nu} \varphi^{\mu\lambda} \varphi_\lambda^\nu, \end{aligned}$$

where $D_\mu = \nabla_\mu - iqA_\mu$, $\varphi \equiv \varphi_\mu^\mu$, and $R_{\nu\rho\lambda}^\mu$ is the Riemann tensor of the background metric. The paprameters q is the charge of the massive spin-two fields. We shall set $q = 1$ without loss of generality in the following discussion. An ansatz where $\varphi_{\mu\nu}$ and A_μ depend only on the radial coordinate z are considered and only the two spatial components of φ are turned on

$$\varphi_{xx}(z) = -\varphi_{yy}(z) = \frac{\psi(z)}{\sqrt{2}z^2}, \quad A_\mu dx^\mu = \phi(z) dt, \quad (19)$$

with all other components of $\varphi_{\mu\nu}$ setting to zero, and the real ϕ and ψ . The ansatz (19) satisfies $\varphi = \varphi_\mu = F_{\mu\rho} \varphi_\nu^\rho = 0$. There are only four nonzero terms left in the material action \mathcal{L}_m ⁷

$$\mathcal{L}_m = -\frac{1}{4} F_{\mu\nu} F^{\mu\nu} - |D_\rho \varphi_{\mu\nu}|^2 - m^2 |\varphi_{\mu\nu}|^2 + 2R_{\mu\nu\rho\lambda} \varphi^{*\mu\rho} \varphi^{\nu\lambda}. \quad (20)$$

Using the planar Schwarzschild-AdS ansatz (6), we can get the equations of motion easily⁸

$$\psi''(z) + \psi'(z) \left[\frac{f'(z)}{f(z)} - \frac{\chi'(z)}{2} \right] + \psi(z) \left[\frac{q^2 e^{\chi(z)} \phi(z)^2}{z^4 f(z)^2} - \frac{m^2}{z^4 f(z)} \right] = 0, \quad (21)$$

$$\phi''(z) + \frac{\chi'(z) \phi'(z)}{2} - \frac{2q^2 \phi(z) \psi(z)^2}{z^4 f(z)} = 0, \quad (22)$$

$$\chi'(z) - 2\kappa^2 z \left[\psi'(z)^2 + \frac{q^2 e^{\chi(z)} \phi(z)^2 \psi(z)^2}{z^4 f(z)^2} \right] = 0, \quad (23)$$

$$f'(z) - \frac{f(z)}{z} + \frac{3}{z^3} - \kappa^2 z \left\{ \frac{e^{\chi(z)} \phi'(z)^2}{2} + f(z) \psi'(z)^2 + \frac{\psi(z)^2}{z^4} \left[m^2 + \frac{q^2 e^{\chi(z)} \phi(z)^2}{f(z)} \right] \right\} = 0. \quad (24)$$

⁷ After changing $\varphi_{\mu\nu}$ to $B_{\mu\nu}$, the matter part \mathcal{L}_m of the action for this model is very similar to the one for the CKMWY d-wave model that in the previous section except for the last term $2R_{\mu\nu\rho\lambda} \varphi^{*\mu\rho} \varphi^{\nu\lambda}$.

⁸ We've set the AdS radius $L = 1$ here.

The charge of tensor field was just set to $q = 1$ without losing generality. We can solve these equations of motion by the shooting method which's detail has been introduced in the previous section. Near the asymptotically AdS boundary, the Maxwell field ϕ and tensor field ψ behave as

$$\phi \approx \mu - \rho z, \quad \psi \approx z^{\Delta_-} \psi_- + z^{\Delta_+} \psi_+, \quad (25)$$

where $\Delta_{\pm} = \frac{3 \pm \sqrt{9 + 4m^2}}{2}$ with the stability bound $m^2 \geq 0$. To keep the conformal dimension Δ_+ the same with that of CKMWY d-wave model studied in previous subsection, we would like to consider the mass of tensor field $m^2 = 7/4$, i.e., $\Delta_- = -1/2$ and $\Delta_+ = 7/2$. According to the gauge/gravity dual dictionary, $\langle \mathcal{O}_{xx} \rangle \equiv \psi_+$ is interpreted as the expected value of operator \mathcal{O}_{xx} , and ψ_- is dual to a source for this operator and must vanish. We can also read out the chemical potential μ and the related charge density ρ from the expansion of $\phi(z)$.

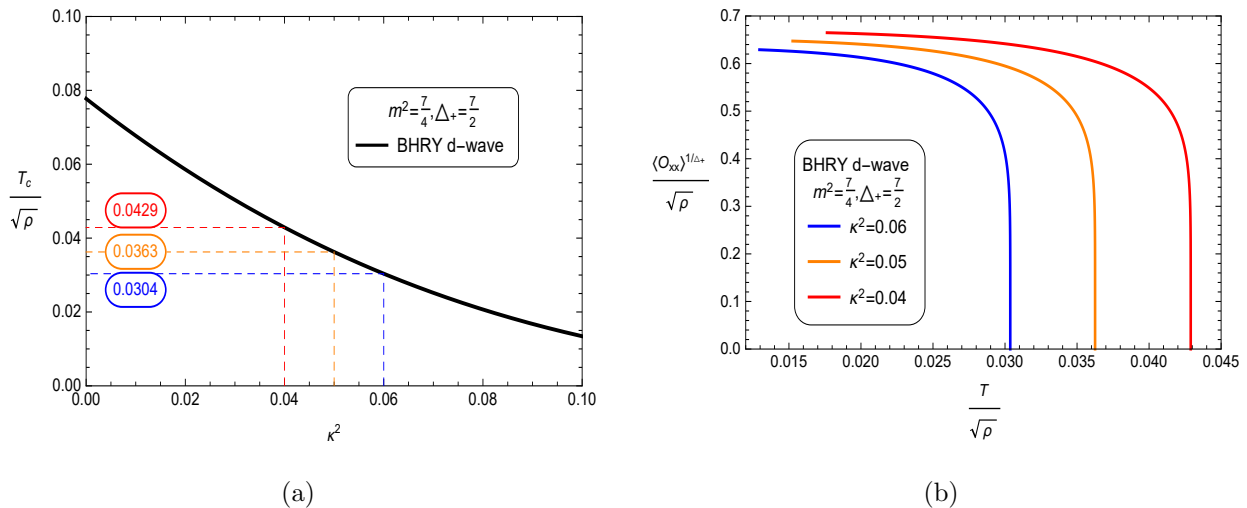


FIG. 2. The left figure depicts the change of critical temperature with backreaction κ^2 for $m^2 = 7/4$ in the BHR d-wave superconducting model. The right figure is the condensate as a function of temperature. Different colors correspond to different backreaction values, the critical temperatures are $T_c/\sqrt{\rho} = 0.0304$ (blue: $\kappa^2 = 0.06$), $T_c/\sqrt{\rho} = 0.0363$ (orange: $\kappa^2 = 0.05$) and $T_c/\sqrt{\rho} = 0.0429$ (Red: $\kappa^2 = 0.04$) respectively. The condensate goes to zero at $T = T_c \propto \sqrt{\rho}$.

In Fig. 2(a), we draw the critical temperature of phase transition with the strength of backreactions κ^2 . The curve in this model is similar to that in CKMWY d-wave model. It is interesting to note that the critical temperature of this d-wave model is slightly smaller than

that of the CKMWY d-wave model (see the blue line), when both the parameters κ and Δ_+ between two models keep the same. Therefore, we can conclude that the non-zero curvature term $2R_{\mu\nu\rho\lambda}\varphi^{*\mu\rho}\varphi^{\nu\lambda}$ in the action (20) makes the superconducting phase transitions more difficult. In Fig. 2(b), we also investigated the condensations of the operator $\langle\mathcal{O}_{xx}\rangle$ for three difference backreactions. Near the critical temperature, the expected value of the operator behaves like $\langle\mathcal{O}_{xx}\rangle\sim(T_c-T)^{1/2}$, which is a second order phase transition.

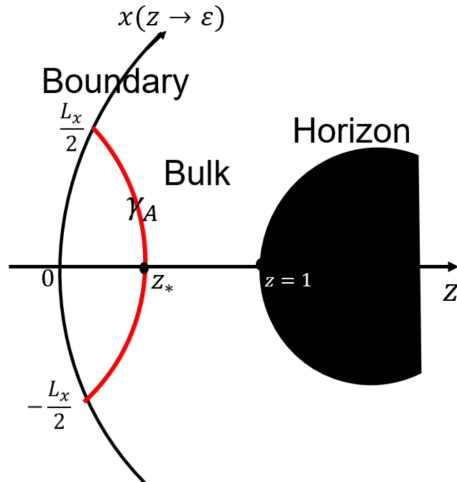


FIG. 3. $\gamma_{\mathcal{A}}$ is the minimum surface of the strip region on the boundary $\mathcal{A}\subseteq[-\frac{L_x}{2},\frac{L_x}{2}]$

III. HEE AND HSC FOR D-WAVE HOLOGRAPHIC SUPERCONDUCTORS

In this section, we will numerically study the HEE and HSC for a strip subregion of the 2-dimensional boundary system for the CKMWY and BHRY d-wave superconducting models. When fixing the time, we can easily obtain the induced metric from the linear element (6)

$$ds_{induced}^2 = \left[\frac{1}{z^4 f(z)} \left(\frac{dz}{dx} \right)^2 + \frac{1}{z^2 L^2} \right] dx^2 + \frac{1}{z^2 L^2} dy^2. \quad (26)$$

Then the area for a strip subsystem \mathcal{A} with the range $x\subseteq[-\frac{L_x}{2},\frac{L_x}{2}]$ and $y\subseteq[-\frac{L_y}{2},\frac{L_y}{2}]$ in Fig. 3 can be given by following formula

$$Area(\mathcal{A}) = 2L_y \int_0^{\frac{L_x}{2}} \frac{dx}{z^3} \sqrt{\frac{1}{f} \left(\frac{dz}{dx} \right)^2 + z^2}. \quad (27)$$

The area of the minimal surface $\gamma_{\mathcal{A}}$ can be obtained by making variation of the integrand function above, and the HEE can be obtained by the RT formula (1). Taking the variational of integrand function (27) with respect to x and considering the boundary condition $\frac{dz}{dx}|_{z=z_*} = 0$, the following integral equation can be derived

$$\frac{dz}{dx} = \sqrt{\frac{f(z_*^4 - z^4)}{z^2}}, \quad (28)$$

where z_* is the turning point of the minimal surface. There is another boundary condition whose boundary is the regular boundary of the asymptotic infinity $z \rightarrow 0$

$$\int_{\varepsilon \rightarrow 0}^{z_*} \frac{z dz}{\sqrt{f(z_*^4 - z^4)}} = \frac{L_x}{2}, \quad (29)$$

where ε is a UV cut off which used to avoid the divergent problem and will be taken a small value in our numerical strategy. Substituting Eq. (28) into Eq. (27) and using the RT formula (1). We can get the total HEE \mathcal{S}

$$\mathcal{S} = \frac{2L_y}{4G_N} \int_{\varepsilon}^{z_*} \frac{z_*^2 dz}{z^3 \sqrt{f(z_*^4 - z^4)}} = \frac{L_y}{2G_N} \left(S_u + \frac{1}{\varepsilon} \right), \quad (30)$$

where S_u is the universal term which is physically important. $1/\varepsilon$ is divergent term which comes from pure AdS background and can be removed by the regularization where the computational details are included in the Appendix A. From Eq. (28), we can also get the integral expression $x(z)$ with respect to z for a minimal surface

$$x(z) = \int_z^{z_*} \frac{z dz}{\sqrt{f(z_*^4 - z^4)}}. \quad (31)$$

The volume enclosed by the minimal surface $\gamma_{\mathcal{A}}$ and the strip region \mathcal{A} can be obtained from the volume integration of the minimal surfaces in the bulk

$$V(\gamma_{\mathcal{A}}) = 2L_y \int_{\varepsilon}^{z_*} \frac{x(z) dz}{z^4 \sqrt{f}}. \quad (32)$$

Using Eq.(2), we can obtain the total HSC

$$\mathcal{C} = \frac{2L_y}{8\pi LG_N} \int_{\varepsilon}^{z_*} \frac{x(z) dz}{z^4 \sqrt{f}} = \frac{L_y}{4\pi LG_N} \left[C_u + \frac{\mathcal{F}(z_*)}{\varepsilon^2} \right], \quad (33)$$

where C_u is the universal term and $\mathcal{F}(z_*)/\varepsilon^2$ is the diverging term. The divergence term comes from the pure AdS background where the computational details are included in the Appendix. Although the divergent term does not have exact expression, we can still solve it numerically. Since the finite term does not change with the cutoff ε , we can subtract the

complexity from each other that corresponding to two different cutoff ε_1 and ε_2 , so that the finite term can be eliminated and $\mathcal{F}(z_*)/(\varepsilon_1^2 - \varepsilon_2^2)$ will be left, where the numerator $\mathcal{F}(z_*)$ of the divergent term will be obtained by numerically. Under the scaling symmetries of Eq. (16), we can rescale the L_x , S_u and C_u as

$$L_x \rightarrow b^{-1}L_x, \quad S_u \rightarrow bS_u, \quad C_u \rightarrow bC_u. \quad (34)$$

Therefore, the dimensionless forms of these quantities are useful

$$L_x\sqrt{\rho}, \quad \frac{S_u}{\sqrt{\rho}}, \quad \frac{C_u}{\sqrt{\rho}}. \quad (35)$$

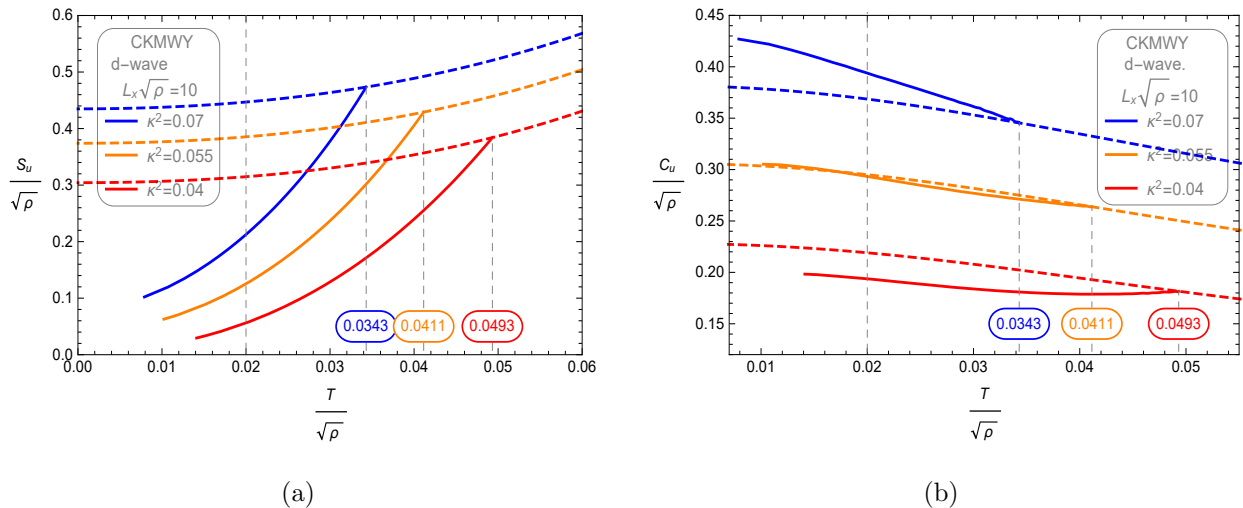


FIG. 4. The HEE (a) and the HSC (b) as functions of the temperature $T/\sqrt{\rho}$ for the CKMWY d-wave superconductor with a fixed subregion L_x : $L_x\sqrt{\rho} = 10$. The dashed and solid curves correspond respectively to normal and superconducting phases.

In Figs. 4 and 5, we plot the HEE and HSC as functions of temperature $T/\sqrt{\rho}$ for two holographic d-wave superconducting models when the strip-width of subregion L_x is fixed. From sub-figure (a) of Figs. 4 and 5, we notice that the HEE increases with the increase of temperature, because the slope of HEE as the temperature is roughly analogous to a specific heat which is natural for it to be positive. In addition, we also find that the HEE increases with the increase of the backreactions κ^2 for a fixed temperature. When considering the effects of non-zero backreactions, we can see that the HEE of the superconducting phase is always lower than that of the normal phase for a given temperature T below the critical point. As the degrees of freedom condense below the critical temperature, the entropy

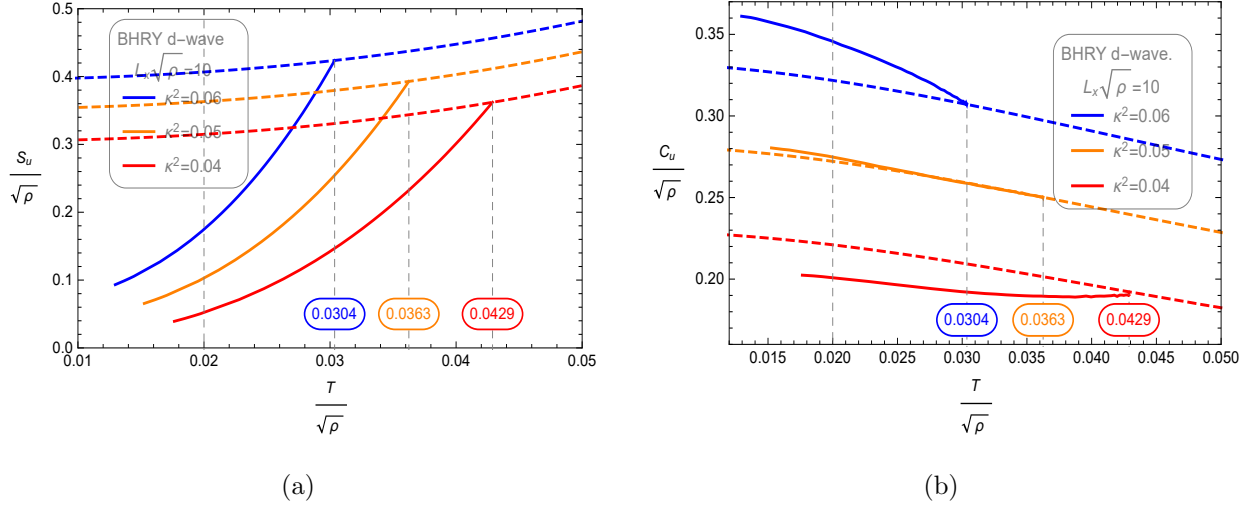


FIG. 5. The HEE (a) and the HSC (b) as functions of the temperature $T/\sqrt{\rho}$ for the BHRy d-wave superconductor with a fixed subregion L_x : $L_x\sqrt{\rho} = 10$. The dashed and solid curves correspond respectively to normal and superconducting phases.

exhibits a lower value, which is similar to the result of s-wave superconductors [31, 32]. It is also noted that there is the slope discontinuity at the point of critical temperature T_c which suggests that the HEE can also be used as an independent probe for d-wave superconducting phase transitions not just in s-wave and p-wave superconductors. We note that the behaviors of the HEE for these two d-wave superconducting models are very similar except for the difference of transformation temperature.

The HSC of the two d-wave superconducting models is shown separately in the second subfigure (b) of Figs. 4 and 5. We find that the slope of the HSC with temperature is discontinuous at the critical point T_c , which means that the HSC can also be used to probe the critical temperature T_c of d-wave superconducting phase transition. Different from the behavior of the HEE, the behaviors of the HSC are more complicated. Specifically, we observe that the behaviors of the HSC for d-wave superconductors depend on both the strip-width $L_x\sqrt{\rho}$ of subregion and the backreactions κ . When $L_x\sqrt{\rho}$ takes some values (like $L_x\sqrt{\rho} = 5$ in Fig. 6) smaller than the critical value or the backreactions κ^2 larger than the critical value, (these critical values of the strip-width are given in the subfigure (b) of Figs. 7 and 8), the superconducting phase always has a larger complexity than the normal phase below the critical temperature. At this time, the HSC C_u for superconducting phase decreases with the increase of temperature $T/\sqrt{\rho}$, which is similar to the result in Ref [31].

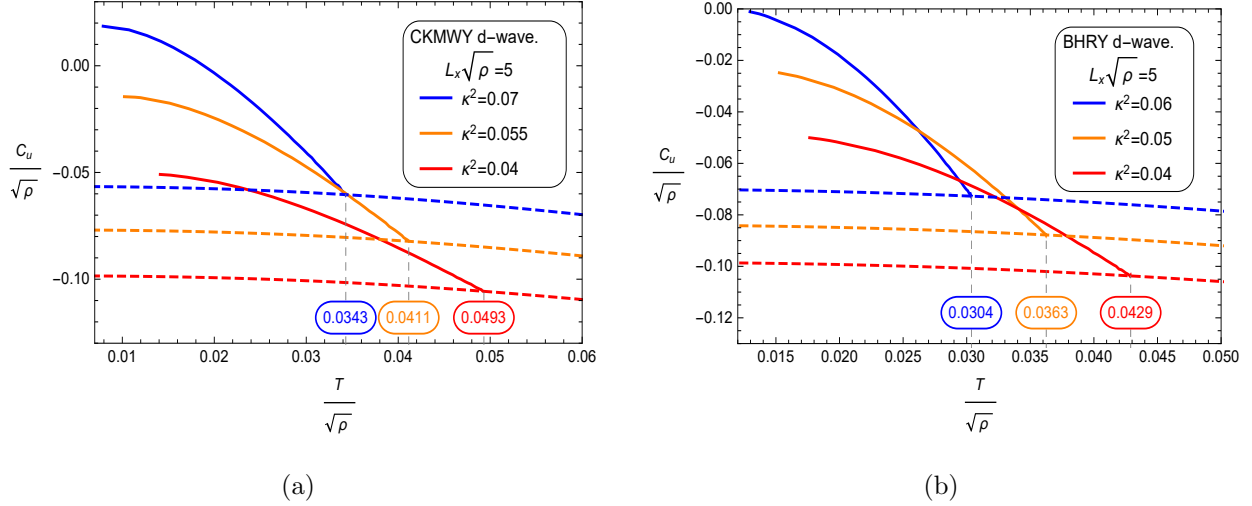


FIG. 6. The HSC as functions of the temperature $T/\sqrt{\rho}$ for the CKMWY (a) and the BHRy d-wave superconductor (b) with a fixed subregion L_x : $L_x\sqrt{\rho} = 5$. The dashed and solid curves correspond respectively to normal and superconducting phases.

When $L_x\sqrt{\rho}$ takes some values (such as $L_x\sqrt{\rho} = 10$ in our Figs. 4 and 5) larger than the critical value and the backreactions κ^2 smaller than the critical value (such as the red line with $\kappa^2 = 0.04$ in our Figs. 4 and 5), we find that the HSC first decreases and then increases slightly as we lower the temperature during the superconducting phase, which is similar to the result of $(2+1)$ -dimensional holographic \mathcal{O}_1 order superconductor in Ref. [32]. The similar phenomena that the different behaviors of the HSC for different fixed strip-widths in superconducting phase transitions has also been found recently in Refs. [38, 39], but the physical mechanism is still unknown.

Furthermore, in the Figs. 7 and 8, we also investigate the HEE and HSC as a function of the strip-width $L_x\sqrt{\rho}$ with the fixed temperature $T/\sqrt{\rho} = 0.02$. We find that both HEE and HSC increases linearly with the increase of strip-width for larger values of $L_x\sqrt{\rho}$. This is known as the “area law”. As we mentioned before, we can see intuitively in the subfigure (b) of Figs. 7 and 8 that there is a crossing point between the HSC of the superconducting phase and that of the normal phase. The behaviors of both HEE and HSC for these two d-wave superconducting models are very similar except for the difference of transformation temperature.

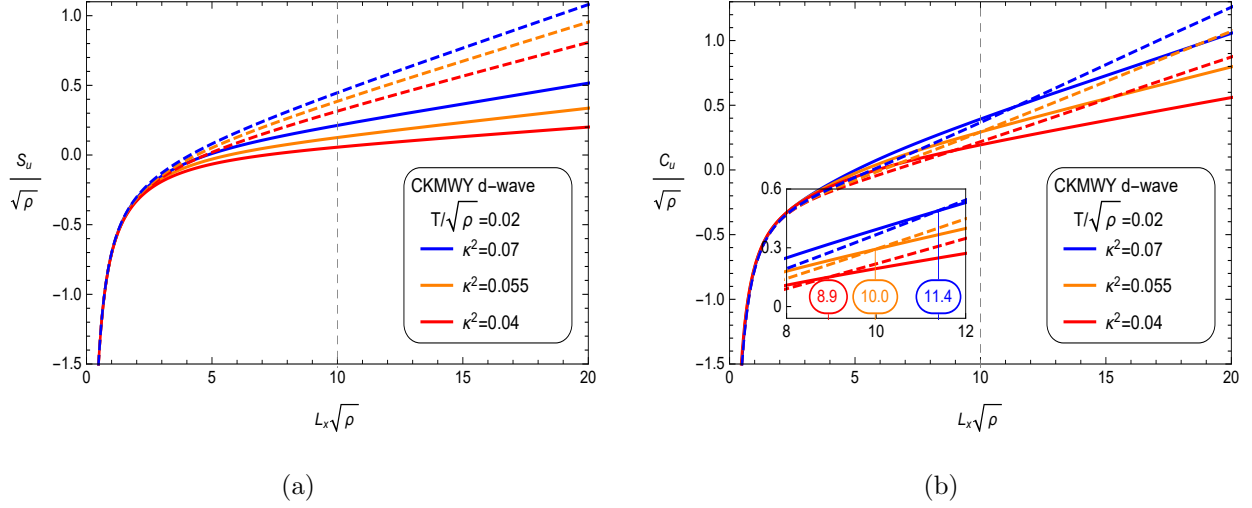


FIG. 7. The HEE (a) and the HSC (b) as functions of the strip-width $L_x\sqrt{\rho}$ for the CKMWY d-wave superconductor with a fixed temperature T : $T/\sqrt{\rho} = 0.02$. The dashed and solid curves correspond respectively to normal and superconducting phases.

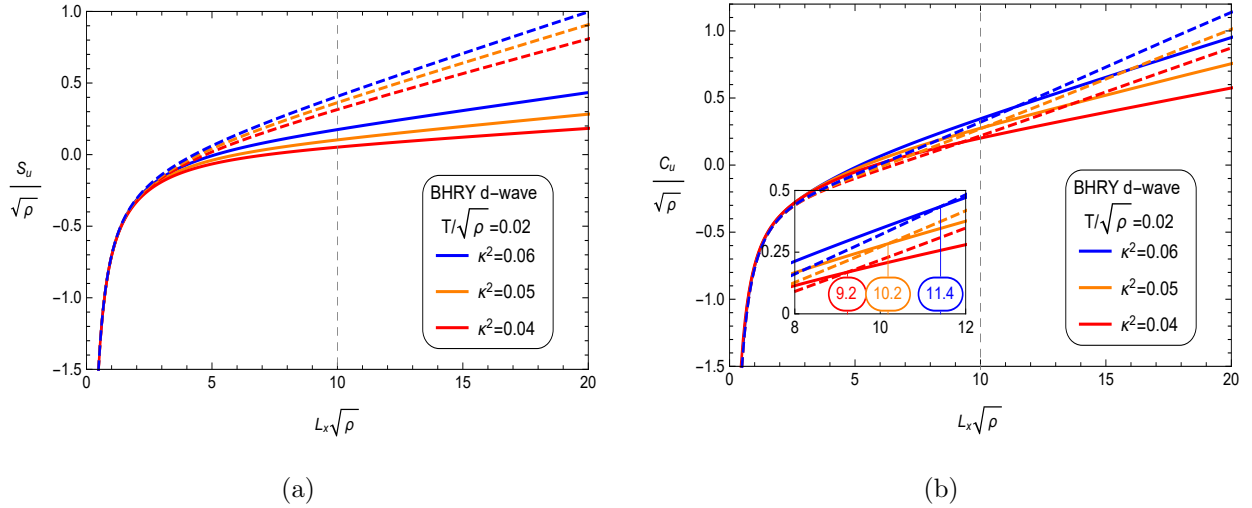


FIG. 8. The HEE (a) and the HSC (b) as functions of the strip-width $L_x\sqrt{\rho}$ for the BHRY d-wave superconductor with a fixed temperature T : $T/\sqrt{\rho} = 0.02$. The dashed and solid curves correspond respectively to normal and superconducting phases.

IV. SUMMARY

In this paper, we investigated the HEE and HSC of two holographic d-wave superconducting models with backreactions. Firstly, we studied condensation characteristics of these two d-wave models after phase transition. By using the same ansatz and keeping the same

dimensions of operators, we obtained the critical temperatures of phase transitions under different backreactions, which shows that the critical temperature decreases as the backreaction increases. This indicates that the backreaction will hinder the d-wave condensation to be formed. It's also worth noting that, when keeping both the parameters κ and Δ_+ corresponding to two models the same respectively, the critical temperature of BHR model is slightly smaller than that of CKMWY model. Further analysis revealed that this slight but important difference is due to the coupling term of tensor field and curvature in the action 19. Secondly, we studied the HEE and HSC for these two holographic d-wave superconducting models. When the strip-widths L_x of subregions were fixed, we found that the slope of HEE and HSC varies with temperature is discontinuous at the point of critical temperature, which means that both the HEE and HSC can be used as good probes to the phase transition in holographic d-wave superconductors. Furthermore, when the temperature was fixed, we observed that the HEE and HSC show similar linear growth behavior for large widths of subregions. We also noted that the d-wave superconducting phase always has a lower HEE than the normal phase due to the condensation of degrees of freedom below the critical temperature. However, the behaviors of HSC are more complicated. More specifically, we found that the behaviors of HSC depend on the strip-width of subregion and the backreaction. When the width of subregion is smaller than a critical value or the backreaction is larger than a critical value, the HSC of the superconducting phase is larger than that of the normal phase. In this case, the HSC decreases with the increase of the temperature which similar to the result in the Ref. [31]. But if the width of subregion is larger than the critical value and the backreaction is smaller than the critical value, the HSC of the superconducting phase is smaller than that of the normal phase. In this case, the HSC first decreases and then increases slightly as we lower the temperature during the superconducting phase, which is similar to the result of $(2+1)$ -dimensional holographic \mathcal{O}_1 order superconductor in Ref. [32]. It shows that the HSC has potential to offer much richer physical information than the HEE although the physical mechanisms involved are still unclear. It's needs to be emphasize that we only focus on the "CV" conjecture of subregion. It's interesting and necessary to use "CA" conjecture and general "CV" conjecture to study the holographic complexity in the holographic superconducting systems.

Appendix A: the HEE and HSC for the normal phase

In this appendix, we shall discuss the diverging term of the HEE and HSC for a strip-shaped subregion $\mathcal{A} \subseteq (-L_x/2 \leq x \leq L_x/2, -L_y/2 \leq y \leq L_y/2)$. For simplicity, let's set $L = 1$ for the rest of calculation. At the normal phase, the solution is simply the RN-AdS solution

$$f(z) = \frac{1}{z^2} - z + \frac{(z^2 - z)\kappa^2\rho^2}{2}, \quad \phi(z) = (1 - z)\rho. \quad (\text{A1})$$

In the probe limit $\kappa^2 \rightarrow 0$, i.e., in the absence of backreaction, since the integration (30) cannot be solved, we can take subregion $L_x \rightarrow 0$, i.e., the minimal surface near the boundary $z \rightarrow 0$. In this case, the metric function has a simple behavior $f(z) \rightarrow 1/z^2$, and then the integral (30) becomes integrable. Therefore, the total HEE for a small subsystem in pure AdS background is obtained

$$\begin{aligned} \mathcal{S} &= \frac{2L_y}{4G_N} \int_{\epsilon}^{z_*} \frac{z_*^2 dz}{z^3 \sqrt{f(z_*^4 - z^4)}} = \frac{L_y}{2G_N} \int_{\epsilon}^{z_*} \frac{z_*^2 dz}{z^3 \sqrt{\frac{1}{z^2}(z_*^4 - z^4)}} \\ &= \frac{L_y}{2G_N} \left(\frac{1}{\epsilon} - \frac{\sqrt{\pi}\Gamma(\frac{3}{4})}{z_*\Gamma(\frac{1}{4})} \right), \end{aligned} \quad (\text{A2})$$

where $1/\epsilon$ is the divergent term caused by the pure AdS background and Γ is the gamma function. Therefore, for all 4-dimensional asymptotic AdS black holes, the total HEE can be expressed in the general form

$$\mathcal{S} = \frac{L}{2G_N} \left(\mathcal{S}_u + \frac{1}{\epsilon} \right), \quad (\text{A3})$$

where \mathcal{S}_u is the universal term of total HEE which is physical important for asymptotic AdS black holes. Considering the same approximation, we can also solve the integral of the minimal surface in the Eq. (31)

$$\begin{aligned} x(z) &= \int_z^{z_*} \frac{z dz}{\sqrt{f(z_*^4 - z^4)}} = \int_z^{z_*} \frac{z dz}{\sqrt{\frac{1}{z^2}(z_*^4 - z^4)}} \\ &= z_* \left\{ \text{EllipticE}(-1) - \text{EllipticK}(-1) + \text{EllipticF} \left[\text{ArcSin} \left(\frac{z}{z_*} \right), -1 \right] \right\} \\ &\quad - z_* \left\{ \text{EllipticE} \left[\text{ArcSin} \left(\frac{z}{z_*} \right), -1 \right] \right\}, \end{aligned} \quad (\text{A4})$$

where *EllipticE*, *EllipticK*, and *EllipticF* are the second, first complete elliptic integrals, and first elliptic integrals respectively. Using the Eq. (33), the total HSC for a small

subsystem in pure AdS background is obtained

$$\begin{aligned} \mathcal{C} &= \frac{2L_y}{8\pi LG_N} \int_\epsilon^{z_*} \frac{x(z)dz}{z^4\sqrt{f}} = \frac{L_y}{4\pi LG_N} \int_\epsilon^{z_*} \frac{x(z)dz}{z^4\sqrt{\frac{1}{z^2}}} \\ &\approx \frac{L_y}{4\pi LG_N} \left\{ \frac{z_*}{2\epsilon^2} [EllipticE(-1) - EllipticK(-1)] - \frac{EllipticK(-1)}{2z_*} + \mathcal{O}(\epsilon) \right\}, \end{aligned} \quad (\text{A5})$$

where $\frac{\mathcal{F}(z_*)}{\epsilon^2}$ is the divergent term of the total HSC caused by the pure AdS background. For different cases, the numerators $\mathcal{F}(z_*)$ of the divergent terms have different forms, but we can still get them numerically. Therefore, for all 4-dimensional asymptotic AdS black holes, the total HSC can be expressed in the general form

$$\mathcal{C} = \frac{L_y}{4\pi LG_N} \left[C_u + \frac{\mathcal{F}(z_*)}{\epsilon^2} \right], \quad (\text{A6})$$

where C_u is the universal term of the total HSC which is physical important for asymptotic AdS black holes.

ACKNOWLEDGMENTS

We thank Prof. Qiu Taotao of Huazhong University of Science and Technology, and Dr. Shi Jiaming of Hangzhou Institute for Advanced Study for their helpful discussions and suggestions. This work was supported by the National Natural Science Foundation of China under Grants No. 11653002 and No. 11875141, and Postgraduate Scientific Research Innovation Project of Hunan Province (Grant No. CX20210472).

-
- [1] J. M. Maldacena, *Adv. Theor. Math. Phys.* **2**, 231 (1998), arXiv:hep-th/9711200.
 - [2] S. S. Gubser, I. R. Klebanov, and A. M. Polyakov, *Phys. Lett.* **B 428**, 105 (1998), arXiv:hep-th/9802109.
 - [3] E. Witten, *Adv. Theor. Math. Phys.* **2**, 253 (1998), arXiv:hep-th/9802150.
 - [4] O. Aharony, A. Fayyazuddin, and J. M. Maldacena, *J. High Energy Phys.* **07**, 013 (1998), arXiv:hep-th/9806159.
 - [5] A. Karch and L. Randall, *J. High Energy Phys.* **06**, 063 (2001), arXiv:hep-th/0105132.
 - [6] A. Karch and E. Katz, *J. High Energy Phys.* **06**, 043 (2002), arXiv:hep-th/0205236.
 - [7] S. A. Hartnoll, *Class. Quant. Grav.* **26**, 224002 (2009), arXiv:0903.3246 [hep-th].

- [8] C. P. Herzog, *J. Phys.* **A42**, 343001 (2009), arXiv:0904.1975 [hep-th].
- [9] J. McGreevy, *Adv. High Energy Phys.* **2010**, 723105 (2010), arXiv:0909.0518 [hep-th].
- [10] J. G. Bednorz and K. A. Muller, *Z. Phys.* **B64**, 189 (1986).
- [11] S. S. Gubser, *Phys. Rev.* **D78**, 065034, (2008), arXiv:0801.2977 [hep-th].
- [12] S. A. Hartnoll, C. P. Herzog, and G. T. Horowitz, *Phys. Rev. Lett.* **101**, 031601, (2008), arXiv:0803.3295 [hep-th].
- [13] S. S. Gubser, *Phys. Rev. Lett.* **101**, 191601, (2008), arXiv:0803.3483 [hep-th].
- [14] S. S. Gubser and S. S. Pufu, *J. High Energy Phys.* **11**, 033, (2008), arXiv:0805.2960 [hep-th].
- [15] G. Kotliar and J. Liu, *Phys. Rev.* **B38**, 5142 (1988).
- [16] N. E. Bickers, D. J. Scalapino, and S. R. White, *Phys. Rev. Lett.* **62**, 961 (1989).
- [17] T. Moriya, Y. Takahashi, and K. Ueda, *J. Phys. Soc. Jap.* **59**, 2905 (1990).
- [18] P. Monthoux, A. V. Balatsky, and D. Pines, *Phys. Rev.* **B 46**, 14803 (1992).
- [19] J.-W. Chen, Y.-J. Kao, D. Maity, W.-Y. Wen, and C.-P. Yeh, *Phys. Rev.* **D 81**, 106008, (2010), arXiv:1003.2991 [hep-th].
- [20] F. Benini, C. P. Herzog, R. Rahman, and A. Yarom, *J. High Energy Phys.* **11**, 137, (2010), arXiv:1007.1981 [hep-th].
- [21] G. Velo, *Nucl. Phys.* **B 43**, 389 (1972).
- [22] S. Ryu and T. Takayanagi, *Phys. Rev. Lett.* **96**, 181602, (2006), arXiv:hep-th/0603001.
- [23] S. Ryu and T. Takayanagi, *J. High Energy Phys.* **08**, 045, (2006), arXiv:hep-th/0605073.
- [24] T. Albash and C. V. Johnson, *J. High Energy Phys.* **05**, 079, (2012), arXiv:1202.2605 [hep-th].
- [25] R.-G. Cai, S. He, L. Li, and Y.-L. Zhang, *J. High Energy Phys.* **07**, 027, (2012), arXiv:1204.5962 [hep-th].
- [26] L. Susskind, *Fortsch. Phys.* **64**, 24 (2016), arXiv:1403.5695 [hep-th].
- [27] D. Stanford and L. Susskind, *Phys. Rev.* **D 90**, 126007, (2014), arXiv:1406.2678 [hep-th].
- [28] A. R. Brown, D. A. Roberts, L. Susskind, B. Swingle, and Y. Zhao, *Phys. Rev. Lett.* **116**, 191301, (2016), arXiv:1509.07876 [hep-th].
- [29] A. R. Brown, D. A. Roberts, L. Susskind, B. Swingle, and Y. Zhao, *Phys. Rev.* **D 93**, 086006, (2016), arXiv:1512.04993 [hep-th].
- [30] M. Alishahiha, *Phys. Rev.* **D 92**, 126009, (2015), arXiv:1509.06614 [hep-th].
- [31] M. Kord Zangeneh, Y. C. Ong, and B. Wang, *Phys. Lett.* **B 771**, 235 (2017), arXiv:1704.00557 [hep-th].

- [32] A. Chakraborty, *Class. Quant. Grav.* **37**, 065021, (2020), arXiv:1903.00613 [hep-th].
- [33] M. Fujita, *Prog. Theor. Exp. Phys.* **2019**, 063B04, (2019), arXiv:1810.09659 [hep-th].
- [34] R.-Q. Yang, H.-S. Jeong, C. Niu, and K.-Y. Kim, *J. High Energy Phys.* **04**, 146, (2019), arXiv:1902.07586 [hep-th].
- [35] Y. Liu, Q. Pan, and B. Wang, *Phys. Lett.* **B 702**, 94 (2011), arXiv:1106.4353 [hep-th].
- [36] Q. Pan, J. Jing, B. Wang, and S. Chen, *J. High Energy Phys.* **06**, 087, (2012), arXiv:1205.3543 [hep-th].
- [37] X.-H. Ge, S. F. Tu, and B. Wang, *J. High Energy Phys.* **09**, 088, (2012), arXiv:1209.4272 [hep-th].
- [38] Y. Shi, Q. Pan, and J. Jing, *Eur. Phys. J. C* **81.**, 228 (2021).
- [39] Y. Shi, Q. Pan, and J. Jing, *Eur. Phys. J. C* **80**, 1100. (2020).